INRIA

INSTITUT NATIONAL DE RECHERCHE EN INFORMATIQUE ET AUTOMATIQUE

# First Steps Towards Automatic Building of Anatomical Atlases

Gérard Subsol, Jean-Philippe Thirion, Nicholas Ayache

**N° 2216**

Mars 1994

PROGRAMME 4

Robotique,

image

et vision


1994

ISSN 0249-6399

INRIA
SOPHIA ANTIPOLIS

# First Steps Towards Automatic Building of Anatomical Atlases

Gérard Subsol, Jean-Philippe Thirion, Nicholas Ayache

Programme 4 — Robotique, image et vision
Projet Epidaure

Rapport de recherche n ° 2216 — Mars 1994 — 22 pages

**Abstract:** This report presents a general scheme for the building of anatomical atlases. We propose to use specific and stable features, the "crest lines" or ridge lines which are automatically extracted from 3D images by differential geometry operators. We have developed non-rigid registration technics and got encouraging results for the building of a first atlas of the crest lines of the skull based on several CT-Scan images of different patients.

**Key-words:** anatomical atlas, tridimensional medical images, crest lines, non-rigid registration, polynomial transformations

*(Résumé : tsvp)*

Unité de recherche INRIA Sophia-Antipolis
2004 route des Lucioles, BP 93, 06902 SOPHIA-ANTIPOLIS Cedex (France)
Téléphone : (33) 93 65 77 77 – Télécopie : (33) 93 65 77 65

# Premiers pas vers la création automatique d'atlas anatomiques

**Résumé :** Dans ce rapport, nous présentons un cadre général pour la création automatique d'atlas anatomiques. Nous proposons d'utiliser des caractéristiques stables, les "lignes de crête" qui sont automatiquement extraites des images médicales tridimensionnelles par des opérateurs de géométrie différentielle. Nous avons développé un algorithme de mise en correspondance non rigide et obtenu des premiers résultats encourageants pour la construction d'un atlas des lignes de crête du crâne à partir d'images scanner de plusieurs patients.

**Mots-clé :** atlas anatomiques, images médicales tridimensionnelles, lignes de crête, mise en correspondance non-rigide, transformations polynomiales

# 1 Introduction

In order to improve the diagnosis and the therapy planning, the physician needs to compare 3D medical images coming from Computed Tomography, Magnetic Resonance Imagery or Nuclear Medicine [Aya93]. We will not discuss here the problem of multimodality registration but we will still distinguish between three kinds of comparisons:

- comparison of images of the same patient to study the evolution of a disease,
- comparison of images of different patients to contrast a healthy and a pathologic person,
- registration of images with an anatomical atlas.

The aim of anatomical atlas books (for example, [Per83]) is to compile medical observations and give a qualitative description convenient for a skilled physician. In some cases, they can provide us with some quantitative information about the variations among patients as, for instance, the atlas of the brain of Talairach & Tournoux [TT88]. The next step is to use those variability parameters to detect pathologies.

3D medical images are a tremendous opportunity to improve those atlases and to broaden the scope of their applications. However, medical images can be huge (for instance, a CT-Scan of the skull including $144 \times 512 \times 512$ voxels is 18 Mo large); we must therefore develop automatic tools to manage such quantity of data. Furthermore, far better precision can be achieved with 3D image processing technics than with manual ones.

A first attempt to achieve such an electronic atlas for the 3D visualization of organs can be found in [SHP+93]. What we propose is to extend the use of those atlases to the automatic quantification of the variations which could lead to automatic diagnosis and surgical planning.

In this paper, we present our project of an automatical building and use of a quantitative atlas from 3D medical images. After a presentation of the general scheme, we detail the type of features used and also describe precisely a non-rigid registration algorithm. At last, we show some very encouraging results of the automatic building of an atlas of the crest lines extracted from 3D CT-Scan images of skulls, including subgoals such as the automatic determination of the sagittal plane.

## 2 General scheme

Our project may be decomposed into two parts (see figure 1):

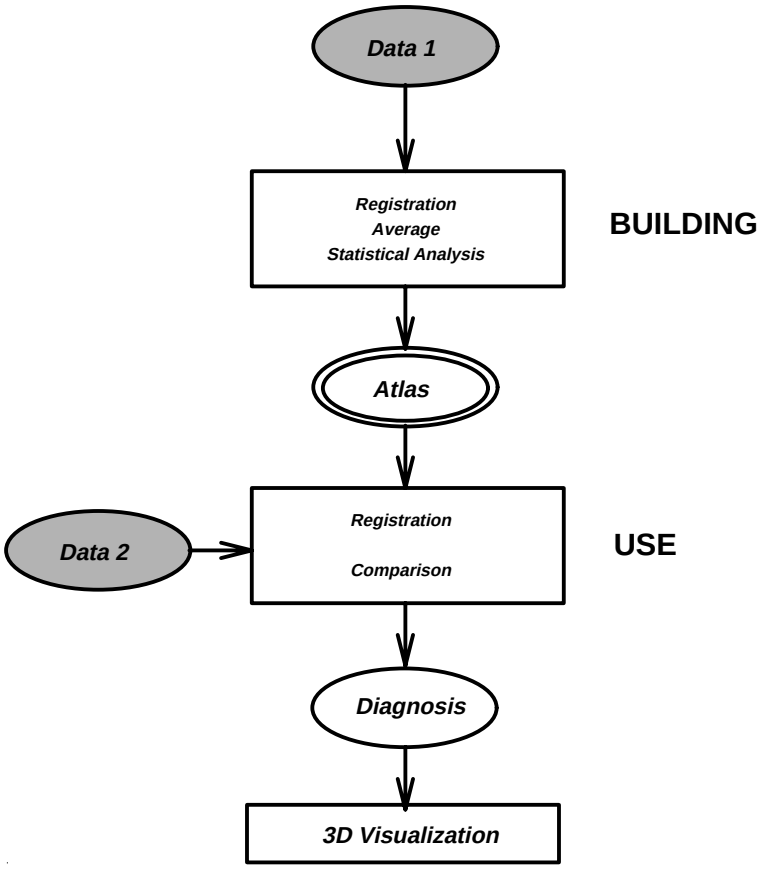


Figure 1: *General scheme*

- *the building*: data 1 is a set of representative objects (for instance, sane patients) which are registered. By making comparisons between the data, the registration algorithm seeks for some features that are shared by this reference set (or a significant subset). The features "average" will then compose the at-

las. A statistical analysis determines the "acceptable difference" in relation to the atlas.

- *the use*: the registration algorithm permits to compare the second set of data, data 2 (for instance, a pathological patient) and the atlas. The statistical parameters give precious information about the level of "abnormality".

In a long-term period, such statistics could be sent to a diagnosis module that could detect some pathologies. For now, we plan to integrate the 3D visualization of the crest lines of the skull and the atlas in the craniofacial surgery simulation testbed developed in the Epidaure project [DSCJ94], in order to help the physician to plan operations.

# 3 The atlas structure

## 3.1 The features

Raw medical images are stored in a discrete 3D matrix $I = f(x, y, z)$. By thresholding $I$, isosurfaces of organs are computed (for instance, the surface of the skull for CT-Scan, of the brain or the face for MRI). The problem is then to compute specific features of these surfaces. Several methods have been proposed to achieve this:

- *surface features*: the mean and Gaussian curvatures are used to segment the isosurface into patches of some fundamental types. Such a decomposition permits to study the deformations of the left ventricle [FMPA92] or to describe the faces [BCR93].
- *line features*: Hosaka [Hos92] reports a wide range of characteristic lines based on differential geometry. The 3D Medial Axis Transform gives also sets of lines, charting for instance the gyral anatomy in [SBK+92].
- *point features*: the "extremal points" [Thi93], based on geometric invariants are used to perform 3D rigid registration.

A first example of a clinical application can be found in Cutting et al. [CBH+93] where line and point features are used in order to compute "an average" skull. In that study however, only semi-automatically extracted features are used.

### 3.2 The crest lines

We decided first to use only line features: the "crest lines" introduced in [TG93]. They are defined as the successive loci of a surface whose largest principal curvature in absolute value is locally maximal in the direction of its principal direction (see figure 2). Let $k_1$ be the principal curvature whose curvature is maximal in absolute value and $\overrightarrow{t_1}$ the associated principal direction, each point of a crest line verifies:

$$\overrightarrow{\nabla}\, k_1 . \overrightarrow{t_1} = 0$$

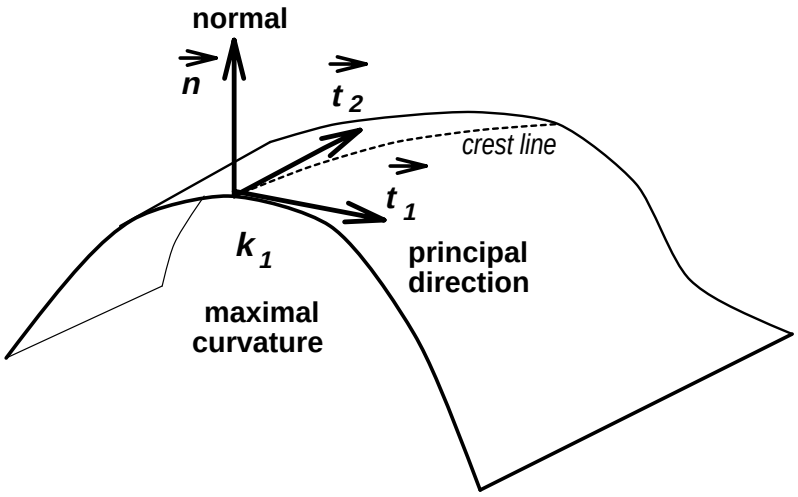


Figure 2: *Differential characteristics of a surface and the crest line.*

These lines are automatically extracted from an isosurface by the "marching lines" algorithm [TG93].

Furthermore, crest lines are anatomically meaningful as emphasized in [BC88]. For instance, in the figure 4, crest lines represent the salient lines of the skull (the orbits, the nose, the mandible, the temples or the cheekbones) and on the brain, the crest lines go along the convolutions.

# 4 The registration algorithm

## 4.1 Previous work

The 3D curves registration algorithm is a key point of our scheme: given two sets $S$ and $S'$ composed of the crest lines $C_i$ and $C'_j$ extracted from images of two different patients, we want to find which lines $C_i$ of $S$ (or portions $P_{i,k}$) correspond to which lines $C'_j$ (or portions $P_{j,l}$) of $S'$ (see figure 3).

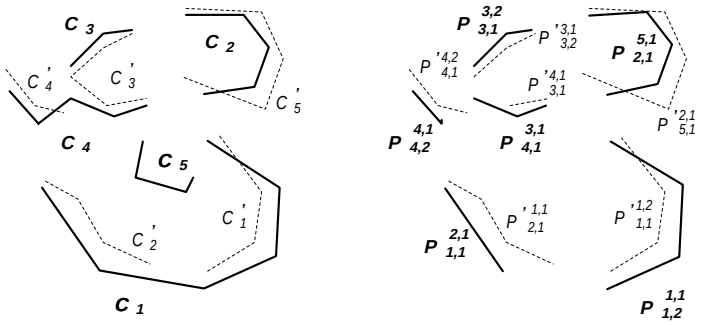


Figure 3: *The registration algorithm has to find the portions $P_{i,k}^{j,l}$ and $P_{j,l}^{'i,k}$, respectively the $k^{th}$ portion of $C_i$ which correspond to the $l^{th}$ portion of $C_j$ and vice versa.*

Two difficulties arise: the number of lines of each set is quite important (from several tens up to several hundreds) and the registration between $S$ and $S'$ is definitely not rigid.

- in [BSSS86] and [SM87], 3D curves matching permits to recognize rigid synthetic objects. First, boundary curves are smoothed and then matched with prestored models but the registration is only rigid.
- in [GA92], the algorithm smoothes curves by using non-uniform B-Splines. Then the two sets of curves are matched with an hashing table indexed by euclidean differential invariants. Results are very good [AGT+93] especially with sets of crest lines but the method only succeeds in finding a rigid displacement and cannot be generalized easily to the non-rigid case.
- Zhang in [Zha92a] and [Zha92b] and independently Besl [BM92] introduced an "iterative closest point" matching method. It consists in three steps:

- for each point $M_i$ of $S$, find the closest point $M'_i$ of $S'$.
- compute the rigid displacement between the two sets of matched points $(M_1 \dots M_n)$ and $(M'_1 \dots M'_n)$ by a least-squares technique.
- apply this motion to $S$ and iterate until the motion is "small".

Both authors use this algorithm to register free-form curves but once again for the rigid case. Nevertheless, we can improve and generalize the method to our problem and our algorithm follows the steps of the "iterative closest point" method.

### 4.2 Points matching

Each point of $S$ is linked with its closest neighbour in $S'$ according to the euclidean distance. We plan also to include in the distance computation differential parameters such as curve tangent, normal, curvature and torsion [GA92] or surface normal, principal directions and principal curvatures as described in [FA94].

Two coefficients are computed with these couples of points: $p_i^j$ and $p_j^{'i}$ which are the proportion of the curve $i$ of $S$ matched with the curve $j$ of $S'$ and vice versa. Thus, by thresholding, $p_i^j \geq thr$ and $p_j^{'i} \geq thr$, we can determine the curves "registered" at $thr$ percent; for instance, the curve $i$ is considered to be definitively registered with the curve $j$ when $p_i^j \geq 0.5$ or $p_j^{'i} \geq 0.5$.

### 4.3 Least-squares transformation

As the registration is not rigid and even not affine, we try to register $S$ and $S'$ with a 2-order polynomial transformation as in [MNR+91] and [Gos88]:

$$\left\{\begin{array}{rcccccccccccc} x' & = & a_1x^2 & +a_2y^2 & +a_3z^2 & +a_4xy & +a_5yz & +a_6xz & +a_7x & +a_8y & +a_9z & +a_{10} \\ y' & = & b_1x^2 & +b_2y^2 & +b_3z^2 & +b_4xy & +b_5yz & +b_6xz & +b_7x & +b_8y & +b_9z & +b_{10} \\ z' & = & c_1x^2 & +c_2y^2 & +c_3z^2 & +c_4xy & +c_5yz & +c_6xz & +c_7x & +c_8y & +c_9z & +c_{10} \end{array}\right.$$

As these polynomials are linear in their coefficients, we can use the least-squares method [PFTV88], [Bjö91] to compute $a_i$, $b_i$ and $c_i$.

We tried to use higher order polynomials but large unexpected undulations then occur as emphasized in [Bro92]. 2-order polynomial transformations give accurate registration but we are not able to decompose them into such intuitive physical meaning transformations as rotation, translation or scaling. Notice that at each iteration, we compose the transformation with a 2-order polynomial and so, we obtain after $n$ iterations a $2^n$-order polynomial transformation.

### 4.4 Updating

The transformation is applied, then the algorithm iterates again or stop according to several criteria:

- *point criterion*: some statistics are computed about the distance distribution between matched points. According for example to the mean value or its variation, we may decide to iterate or to stop. Nevertheless, this criterion is only local and geometric; it is not representative of the real registration between curves.
- *curve criterion*: we can compare the evolution of the registration coefficients $p_i^j$ and $p_j^{'i}$ and stop the iterations when they are stable: the curves registration is then in a local minimum.
- *transform criterion*: we compute the matrix norm $|||T - I_d|||$ where $T$ is the transformation and $I_d$ the identity matrix. This parameter evaluates the dynamics of the iteration process.

Furthermore, by incrementing the threshold value *thr* at each iteration, for instance, from 0 to 0.5 by step of 0.025 and by taking only in account the matched point couples $(M, M')$ belonging to registered curves at *thr* percent, the algorithm tends to improve the registration of already matched curves and to discard isolated ones.

### 4.5 Results

First, we applied this algorithm to two sets of the longest crest lines automatically extracted from 3D images of the skulls of two different patients. We initialized the non rigid registration by scaling the two skulls at the same height and by aligning their centroids. We can notice in figure 5 (left) that the number of lines of the two sets (45 and 32 lines) and their shape (notice, in particular, the nose) are different and that the two skulls are quite shifted.

One set of lines $S$ is then deformed to be registered with the second $S'$. To evaluate the result, we display in figure 5 (right) the registered lines of the set $S'$ and of the set $S$ after deformation. The matched points are linked by segments. The registration takes less than three minutes on a DEC-Alpha workstation.

The algorithm detects and matches similar lines (15 lines) as the orbits, the mandible, the temples and the foramen occipitale.

In figure 6, we show (left) the registered lines of the set $S'$ and of the set $S$ not transformed in order to check the accuracy of the algorithm. We display (right) the deformation applied to a regular mesh.

Then, we applied this deformation to the whole set $S$ of crest lines (543 lines) and we run again the algorithm with the whole set $S'$ (543 lines). The result is quite impressive (see figure 7): new similar lines appear as the cheekbones, the top of the mandible. The points matching is also acceptable.

# 5 Some remarks

## 5.1 Initialization

This algorithm is iterative and converges towards a local minimum. So, it depends on the initial position and, in particular, is very sensitive to rotations. A solution as proposed by both Besl and Zhang is to test the matching with a set of initial positions of the shape and to take the best.

We can also use the inertia moments to do a first coarse registration: we compute the inertia matrix of the two sets of curves, then diagonalize it to find the principal axis. As we have only directions, we obtain several basis. Then we register all the basis of the two sets and we choose the matching which minimizes the distances between points. This method is however still sensitive to severe occlusions.

We can also use the natural symmetry of organic objects as the skull. We develop a method to find automatically the symmetry planes:

- apply a symmetry $S$ to the object (for example, $x' = -x$),
- register the object and its symmetric with the algorithm at the order 0 (then, it is very close of the ICP method) and find the rigid transformation $T$.
- from $T$ and $S$, deduce the symmetry plane. In figure 8, we show how the sagittal plan (the vertical symmetry plan) of the skull is automatically found.

By aligning the symmetry planes of the two objects and minimizing the distance between the two centroids, we obtain a quite good initialization.

## 5.2 The order of the 3D transformation

We have studied the accuracy of the transformation according to the order. In the graph 1, we show the distribution function of the distance between matched points

| Order | Min | Max | Mean | Standard Deviation | Median |
|---|---|---|---|---|---|
| 0 (Rigid) | 0.003395 | 0.212321 | 0.056587 | 0.038605 | 0.043657 |
| 1 (Affine) | 0.003121 | 0.200469 | 0.044875 | 0.026226 | 0.038163 |
| 2 | 0.002219 | 0.139956 | 0.031291 | 0.021781 | 0.022436 |

Table 1: Distance between the matched points according to the order.

according to the order 0 (rigid case), 1 (affine case) and 2. The abscissa $x$ represents the distance between two matched points (the coordinates of the two skulls are comprised between -1 and 1). The ordinate $y$ is the percentage of pairs of matched points whose distance is inferior to $x$.

The order 2 is far better than the others with this respect. This is confirmed by the figures of the table 1. The mean value is then 43% lower for the order 2 than order 1 and 81% than the rigid case. The standard deviation is respectively 20% and 77% lower than the order 1 and 0.

### 5.3 Sampling robustness

We made experiments to test the robustness of our algorithm according to the difference of sampling. We sample the curves of $S'$ by taking at random $1/5^{th}$ and $1/10^{th}$ of points. We apply then the registration algorithm. We see in the figure 9 that the registration remains coherent in spite of the non-regular decimation.

## 6 Application: Automatic Labelling

Given $n$ sets of lines, we can register all the sets two by two. Then, we construct a "similarity graph":

- the nodes are the lines $L_i^j$ where $i$ is the number of the set and $j$ the index of the line in the set $S_i$,
- the vertices represent the relation "is registered with".

Now, we search for the connected parts of this graph sharing at least a line of each set. Hence, we determine the subsets of similar lines that compose the "atlas".

We have experienced this method with three sets of crest lines extracted from three CT-Scan images of the skull of different patients. We found 72 subsets of

similar lines and as we labelled some lines of one set, we can estimate the relevance of the subsets in figure 10. Notice that a subset may be composed of several lines of the same set (for example, three lines make up the right temple of the first skull).

# 7 Conclusion

In this paper, we have presented some very encouraging results about the automatically building and use of an anatomical atlas. Now, we are studying the averaging algorithm in order to produce a first atlas of the crest lines of the skull with a larger database of sane and pathological patients. We want also to develop a statistical analysis of the variations as in [CHTH93]. The next step is the integration of this atlas into the craniofacial surgery simulation testbed of our project. We plan also to use the whole scheme to build an atlas of the convolutions of the brain and to compare it with the atlas book [OKA90].

# Acknowledgments

This work was partially supported by Digital Equipment Corporation and the Esprit European project Bra-Viva. We thank General-Electric and Bruce Latimer, Director at the Cleveland Museum of Natural History, Court Cutting, David Dean and André Guéziec for the CT-Scan data of the skulls. Jacques Feldmar gave a substantial help in this work.

## References

[AGT+93] N. Ayache, A. Guéziec, J.P. Thirion, A. Gourdon, and J. Knoplioch. Evaluating 3D Registration of CT-Scan Images Using Crest Lines. In David C. Wilson and Wilson Joseph N., editors, *Mathematical Methods in Medical Imaging II 1993*, pages 29–44, San Diego, California (USA), July 1993. SPIE.

[Aya93] Nicholas Ayache. Volume Image Processing. Results and Research Challenges. Technical Report 2050, INRIA, September 1993.

[BC88] Fred L. Bookstein and Court B. Cutting. A proposal for the apprehension of curving cranofacial form in three dimensions. In K. Vig and A. Burdi, editors, *Cranofacial Morphogenesis and Dysmorphogenesis*, pages 127–140. 1988.

[BCR93] Vicki Bruce, Anne Coombes, and Robin Richards. Describing the shapes of faces using surface primitives. *Image and Vision Computing*, 11(6):353–363, August 1993.

[Bjö91] Å Björck. Algorithms for Linear Least Squares Problems. In Emilio Spedicato, editor, *Computer Algorithms for Solving Linear Algebraic Equations, the State of the Art*, pages 57–92. Springer-Verlag, 1991.

[BM92] Paul J. Besl and Neil D. McKay. A Method for Registration of 3-D Shapes. *IEEE PAMI*, 14(2):239–255, February 1992.

[Bro92] Lisa Gottesfeld Brown. A Survey of Image Registration Techniques. *ACM Computing Surveys*, 24(4):325–376, December 1992.

[BSSS86] C. Marc Bastuscheck, Edith Schonberg, Jacob T. Schwartz, and Micha Sharir. Object recognition by three-dimensional curve matching. *International Journal of Intelligent Systems*, 1:105–132, 1986.

[CBH+93] Court B. Cutting, Fred L. Bookstein, Betsy Haddad, David Dean, and David Kum. A spline-based approach for averaging three-dimensional curves and surfaces. In David C. Wilson and Wilson Joseph N., editors, *Mathematical Methods in Medical Imaging II 1993*, pages 29–44, San Diego, California (USA), July 1993. SPIE.

[CHTH93] T.F. Cootes, A. Hill, C.J. Taylor, and J. Haslam. The Use of Active Shape Models For Locating Structures in Medical Images. In H.H. Barrett and A.F. Gmitro, editors, *Information Processing in Medical Imaging*, pages 33–47, Flagstaff, Arizona (USA), Juin 1993. IPMI'93, Springer-Verlag.

[DSCJ94] Hervé Delingette, Gérard Subsol, Stéphane Cotin, and Pignon Jérôme. A Craniofacial Surgery Simulation Testbed. Technical Report 2199, INRIA, Sophia-Antipolis (France), February 1994.

[FA94] Jacques Feldmar and Nicholas Ayache. Rigid and Affine Registration of Smooth Surfaces using Differential Properties. In *ECCV*, Stockholm (Sweden), May 1994. ECCV. To appear.

[FMPA92] Denis Friboulet, Isabelle E. Magnin, Andreas Pommert, and Michel Amiel. 3D Curvature Features of the Left Ventricle from CT Volumic Images. In *Information Processing in Medical Imaging*, pages 182–192. IPMI'92, 1992.

[GA92] A. Guéziec and N. Ayache. Smoothing and Matching of 3-D Space Curves. In *Visualization in Biomedical Computing*, pages 259–273, Chapel Hill, North Carolina (USA), October 1992. SPIE.

[Gos88] Ardeshir Goshtasby. Image Registration by Local Approximation Methods. *Image and Vision Computing*, 6(4):255–261, November 1988.

[Hos92] M. Hosaka. *Modeling of Curves and Surfaces in CAD/CAM.* Springer-Verlag, 1992.

[MNR+91] Gerald Q. Maguire, Marilyn E. Noz, Henry Rusinek, Judith Jaeger, Elissa L. Kramer, Joseph J. Sanger, and Gwenn Smith. Graphics Applied to Medical Image Registration. *IEEE Computer Graphics & Applications*, pages 20–27, March 1991.

[OKA90] Michio Ono, Stefan Kubik, and Chad D. Abernathey. *Atlas of the Cerebral Sulci.* Georg Thieme Verlag, 1990.

[Per83] Eduard Pernkopf. *Atlas d'anatomie humaine.* Piccin, 1983.

[PFTV88] William H. Press, Brian P. Flannery, Saul A. Teukolsky, and William T. Vettening. *Numerical Recipes in C, The Art of Scientific Computing.* Cambridge University Press, 1988.

[SBK+92] G. Székely, Ch. Brechbühler, O. Kübler, R. Ogniewicz, and T. Budinger. Mapping the human cerebral cortex using 3D medial manifolds. In Richard A. Robb, editor, *Visualization in Biomedical Computing*, pages 130–144, Chapel Hill, North Carolina (USA), October 1992. SPIE.

[SHP+93] R. Schubert, K. H. Höhne, A. Pommert, M. Riemer, Th. Schiemann, and U. Tiede. Spatial Knowledge Representation for Visualization of Human Anatomy and Function. In H.H. Barrett and A.F. Gmitro, editors, *Information Processing in Medical Imaging*, pages 168–181, Flagstaff, Arizona (USA), June 1993. IPMI'93, Springer-Verlag.

[SM87] Jacob T. Schwartz and Sharir Micha. Identification of Partially Obscured Objects in Two and Three Dimensions by Matching Noisy Characteristic Curves. *The International Journal of Robotic Research*, 6(2):29–44, Summer 1987.

[TG93] J.P. Thirion and A. Gourdon. The Marching Lines Algorithm : new results and proofs. Technical Report 1881, INRIA, March 1993.

[Thi93] J.P. Thirion. New feature points based on geometric invariants for 3D image registration. Technical Report 1901, INRIA, May 1993.

[TT88] Jean Talairach and Pierre Tournoux. *Co-Planar Stereotaxic Atlas of the Human Brain*. Georg Thieme Verlag, 1988.

[Zha92a] Zhengyou Zhang. Iterative Point Matching for Registration of free-form curves. Technical Report 1658, INRIA, April 1992.

[Zha92b] Zhengyou Zhang. On Local Matching of Free-Form Curves. In David Hogg and Roger Boyle, editors, *British Machine Vision Conference*, pages 347–356, Leeds (United Kingdom), September 1992. British Machine Vision Association, Springer-Verlag.

Unité de recherche INRIA Lorraine, Technôpole de Nancy-Brabois, Campus scientifique,
615 rue de Jardin Botanique, BP 101, 54600 VILLERS LÈS NANCY
Unité de recherche INRIA Rennes, IRISA, Campus universitaire de Beaulieu, 35042 RENNES Cedex
Unité de recherche INRIA Rhône-Alpes, 46 avenue Félix Viallet, 38031 GRENOBLE Cedex 1
Unité de recherche INRIA Rocquencourt, Domaine de Voluceau, Rocquencourt, BP 105, 78153 LE CHESNAY Cedex
Unité de recherche INRIA Sophia-Antipolis, 2004 route des Lucioles, BP 93, 06902 SOPHIA-ANTIPOLIS Cedex

Éditeur
INRIA, Domaine de Voluceau, Rocquencourt, BP 105, 78153 LE CHESNAY Cedex (France)
ISSN 0249-6399

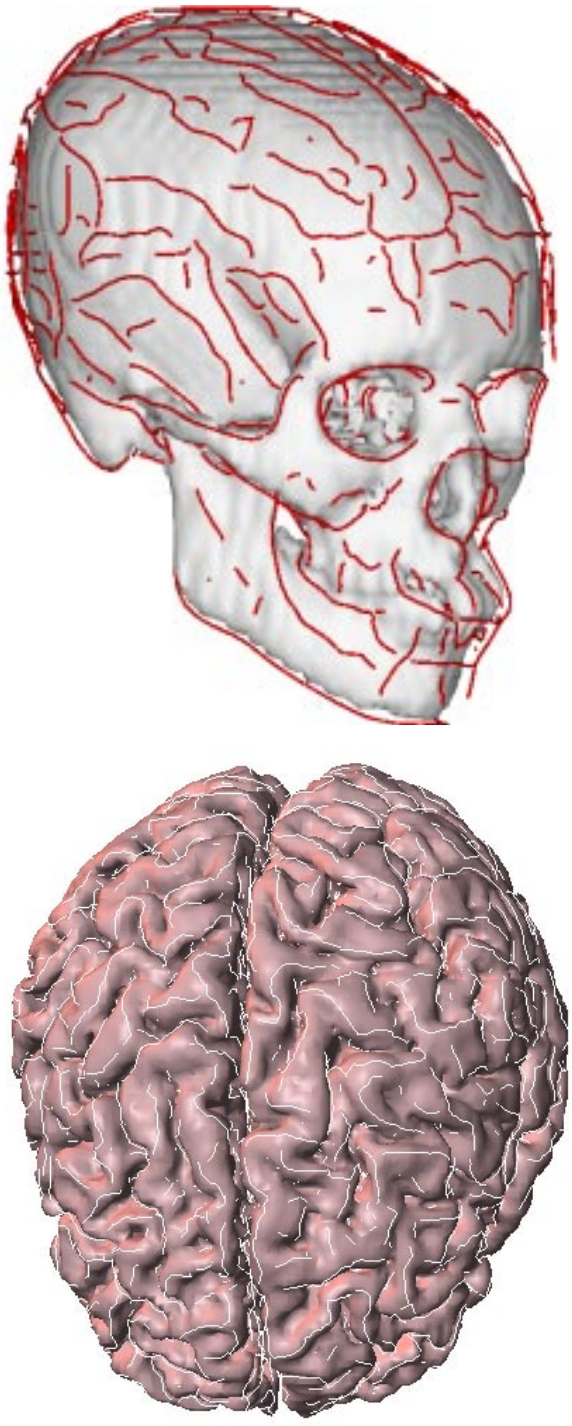



Figure 4: *Crest lines of a skull and of a brain.*

Figure 5: *Left: The longest crest lines of the two skulls superimposed. Right: Registration of similar lines after the deformation.*

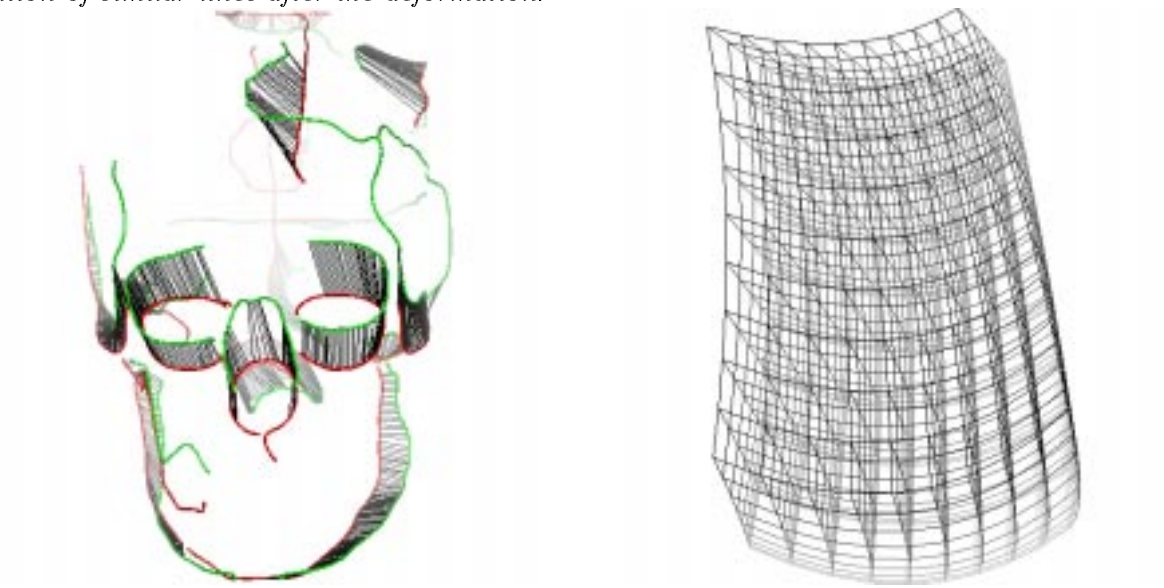

Figure 6: *Left: Registration of similar lines in their original position. Right: The registration deformation applied to a regular mesh.*

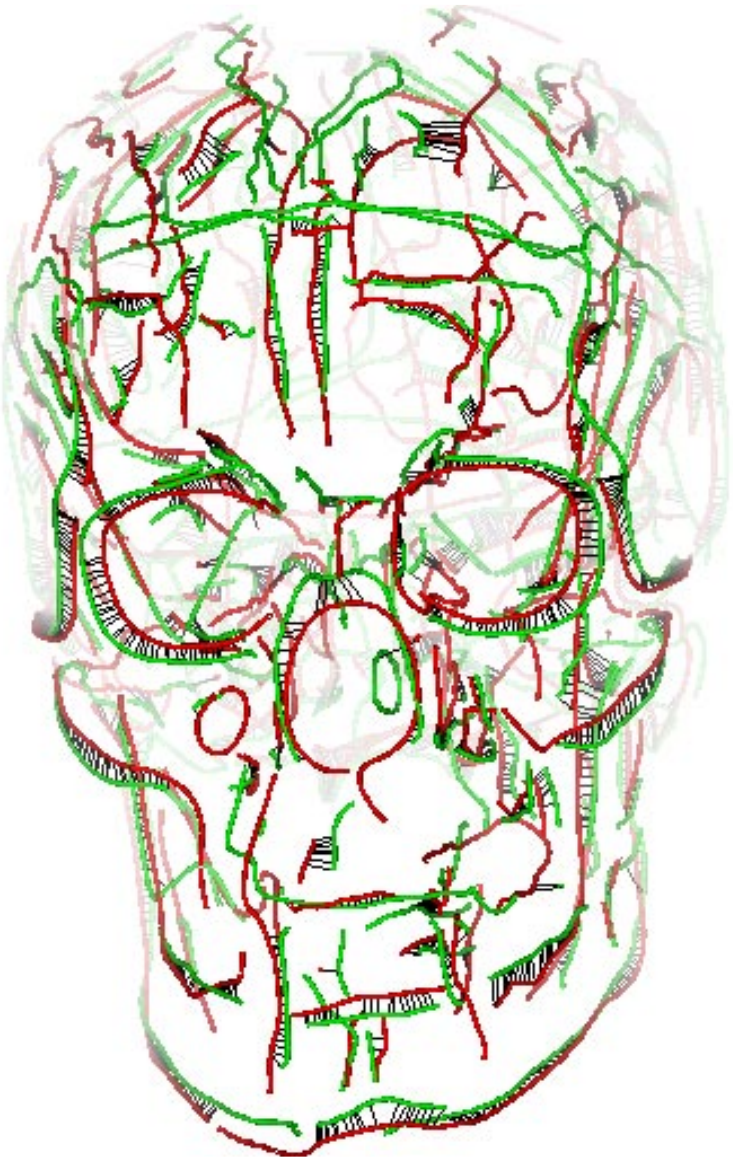

Figure 7: *Registration of two whole sets of crest lines after deformation. Notice the nice registration of the nose, the orbits, the mandible, the temples and the cheekbones.*

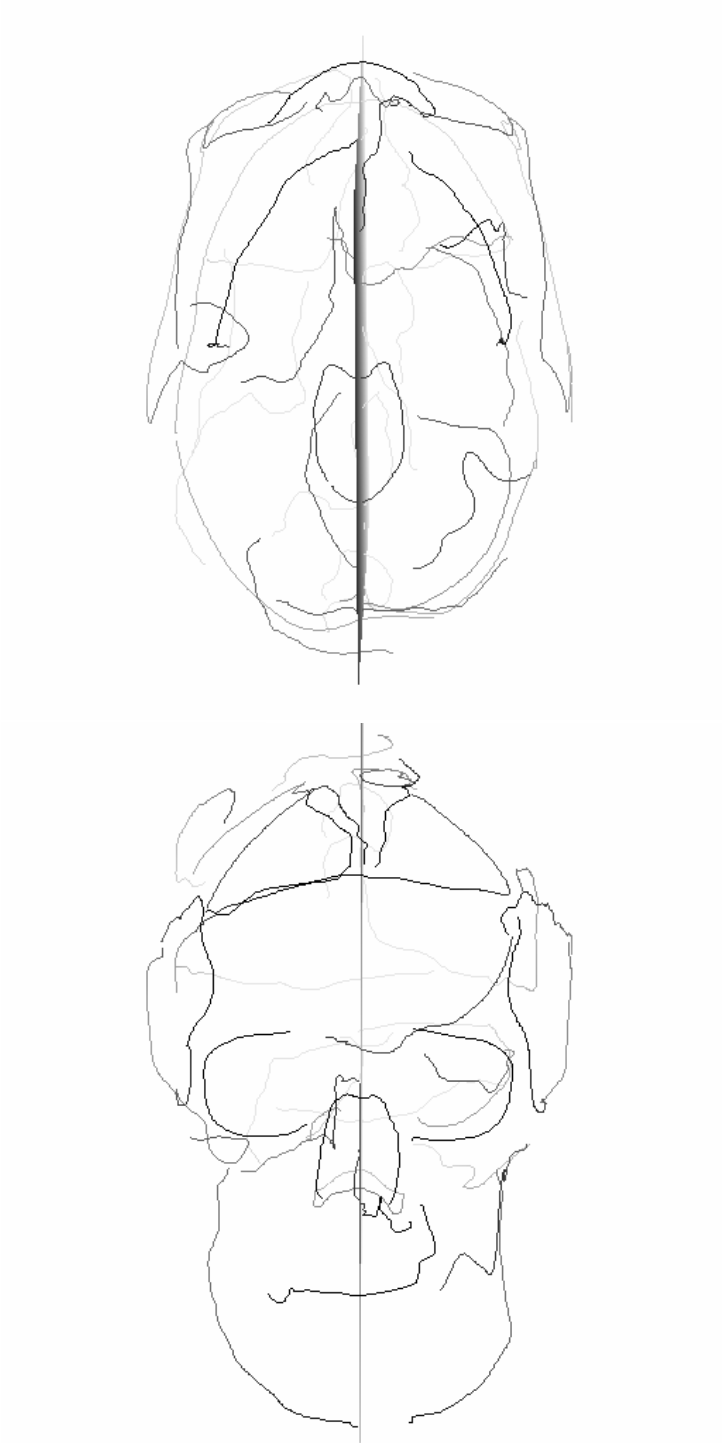



Figure 8: *The sagittal plan of the skull is automatically detected: the plan is displayed as a rectangle in bottom and front views.*

**Graph 1: Distribution function of the distance between matched points**

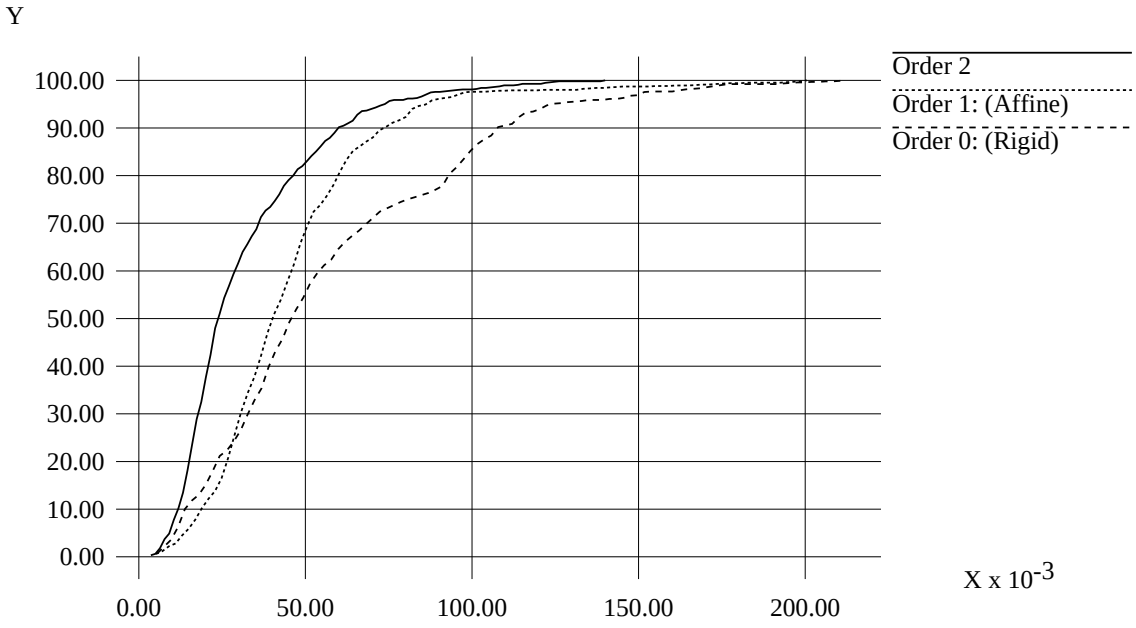

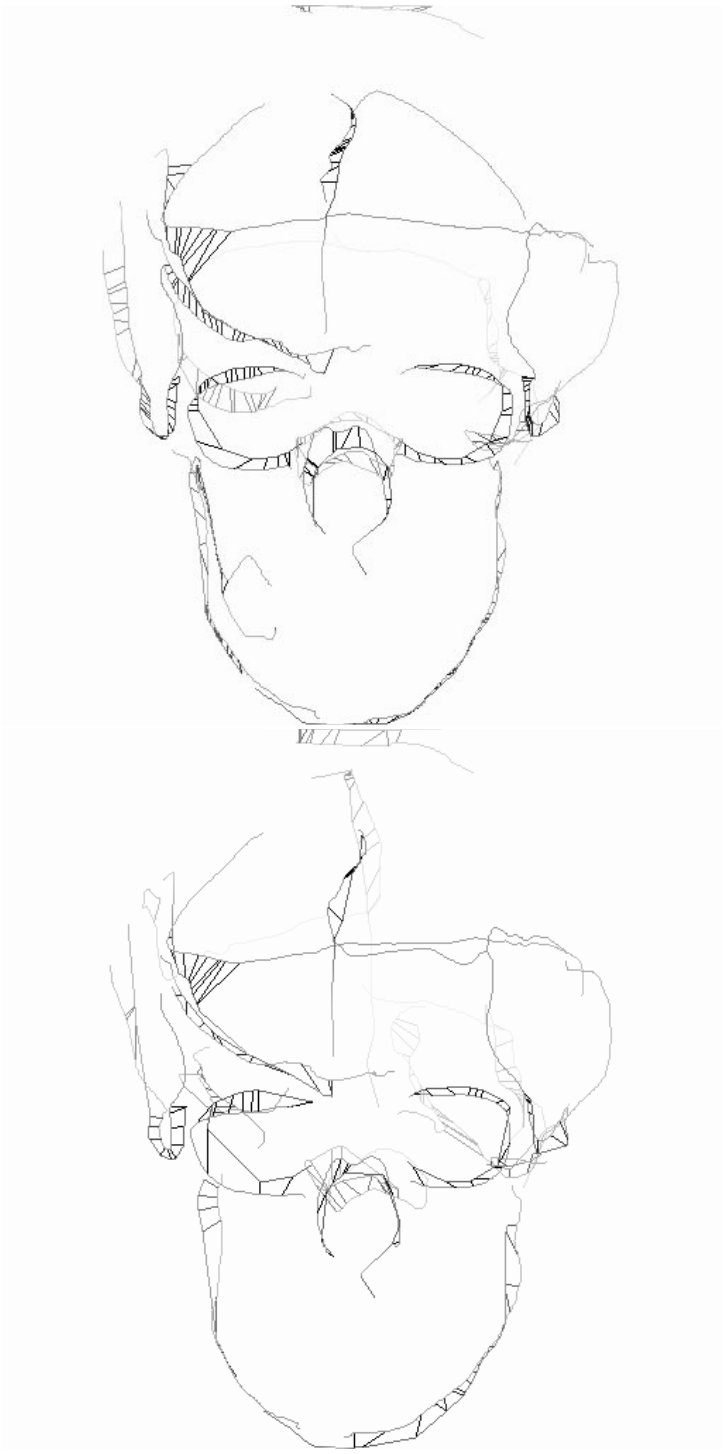



Figure 9: *Registration of two sets of curves differently sampled ($1/5^{th}$ of points sampled at random, up and $1/10^{th}$ of points sampled at random, bottom). The registered curves remain the same and the matched points are coherent.*

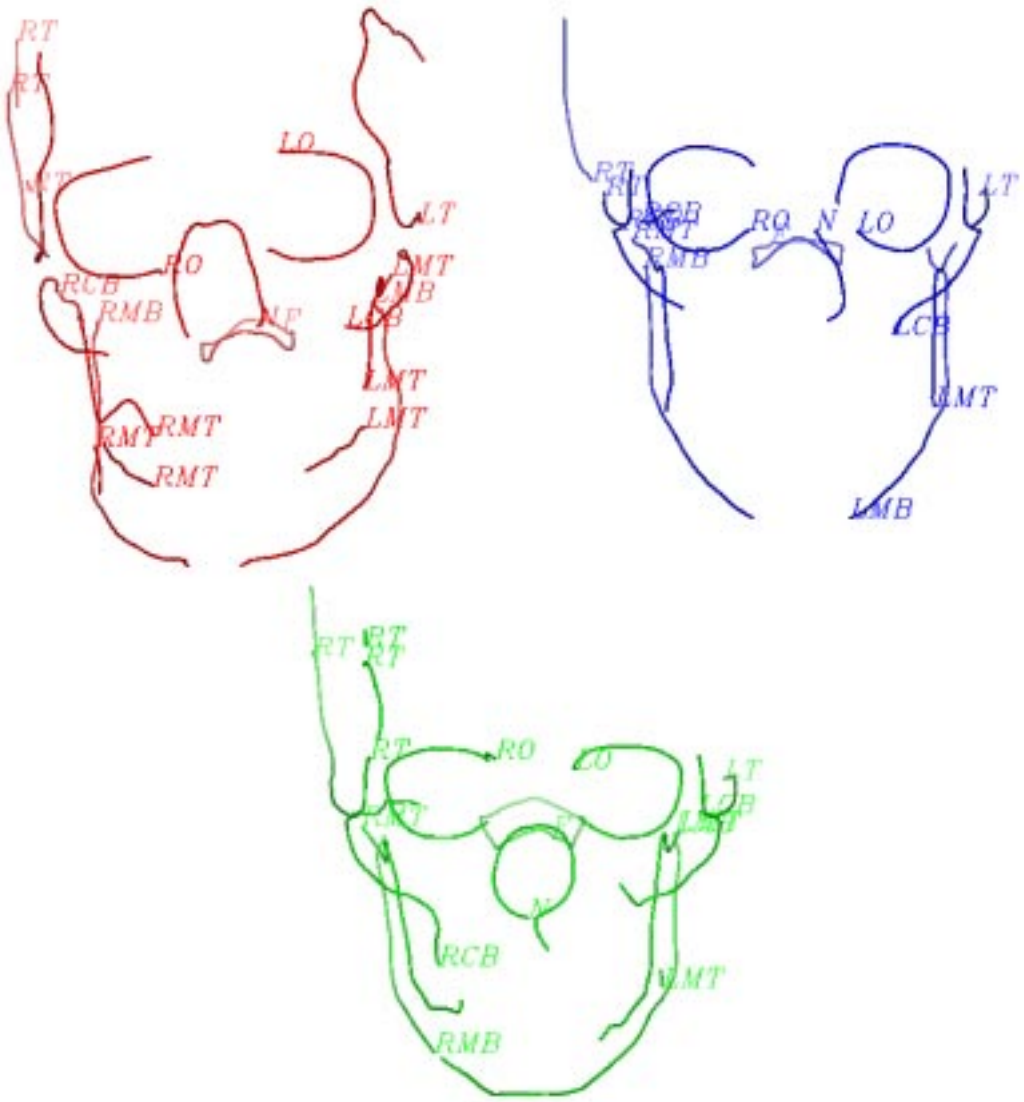


Figure 10: *Automatic labelling of three different skulls: LO=Left Orbit, RO=Right Orbit, LT=Left Temple, RT=Right Temple, LMB & LMT=Left Part of the mandible (Bottom & Up), RMB & RMT=Right Part of the mandible (Bottom & Up), LCB=Left Cheekbone, RCB=Right Cheekbone, F=Foramen Occipitale, N=Nose.*